The Feasibility of Head Motion Tracking in Helical CT: A Step Towards Motion Correction

Jung-Ha Kim,[1] Johan Nuyts,[2,3] Zdenka Kuncic,[4] and Roger Fulton[1,4,5,*]

[1] *Medical Radiation Sciences, University of Sydney, NSW 2141, Australia*
[2] *Department of Nuclear Medicine, Katholieke Universiteit, Leuven, Belgium*
[3] *Medical Imaging Research Center, Katholieke Universiteit, Leuven, Belgium*
[4] *School of Physics, University of Sydney, NSW 2050, Australia*
[5] *Department of Medical Physics, Westmead Hospital, Westmead, NSW 2145, Australia*

(Dated: February 25, 2013)

Purpose: To establish a practical and accurate motion tracking method for the development of rigid motion correction methods in helical x-ray computed tomography (CT).

Methods: A commercially available optical motion tracking system provided 6 degrees of freedom pose measurements at 60 Hz. A 4×4 calibration matrix was determined to convert raw pose data acquired in tracker coordinates to a fixed CT coordinate system with origin at the isocenter of scanner. Two calibration methods, absolute orientation (AO), and a new method based on image registration (IR), were compared by means of landmark analysis and correlation coefficient in phantom images co-registered using the derived motion transformations.

Results: Transformations calculated using the IR-derived calibration matrix were found to be more accurate, with positional errors less than 0.5 mm (mean RMS), and highly correlated image voxel intensities. The AO-derived calibration matrix yielded larger mean RMS positional errors ($\simeq$1.0 mm), and poorer correlation coefficients.

Conclusions: We have demonstrated the feasibility of accurate motion tracking for retrospective motion correction in helical CT. Our new IR-based calibration method based on image registration and function minimization was simpler to perform and delivered more accurate calibration matrices. This technique is a useful tool for future work on rigid motion correction in helical CT and potentially also other imaging modalities.

Key words: computed tomography (CT), head motion, motion artifact, motion tracking

I. INTRODUCTION

Patient motion, which creates inconsistencies within the acquired projection data, is a major source of artifacts in clinical x-ray computed tomography (CT).[1,2] A method of compensating for head motion, which may be considered approximately rigid, in helical CT would be of considerable benefit when imaging children,[3] as well as patients suffering dementia or head trauma.[4] Several retrospective motion correction techniques have been proposed to compensate for head motion.[5–12]. All of these rely on information about motion of the head in the CT coordinate system during the CT scan. Some studies have also proposed methods for motion estimation from the acquired projection data.[5–10] Other studies have proposed rigid motion tracking methods for CT for purposes other than motion correction, such as neurosurgery,[13] or to estimate the magnitude of head motion during helical CT.[14]

Of these existing motion estimation methods, three[8–10] can provide six degrees of freedom (d.o.f.) motion estimates in CT coordinates, and one[14] provides estimates in a coordinate system fixed to the bed.

Jacobson and Stayman,[8] and Bhowmik *et al.*[9] derived motion estimates in cone beam CT by identifying radio-opaque markers in each projection. Bodensteiner *et al.*[10] evaluated an image registration method to correct for small rigid motions, such as C-arm positioning errors due to mechanical flexing. Wagner et al.[14] did not evaluate the quantitative accuracy of derived motion estimates. However this method could potentially be adapted to give estimates directly in CT coordinates, using knowledge of bed position, and is a potential alternative to the method described here. Another promising approach by Katsevich et al.[15] provides estimates of local motion in cardiac CT using an empirical measure of image clutter termed edge entropy. Since local motion estimation is a more challenging problem than rigid motion estimation, it may well be possible to adapt this method to rigid motion.

Therefore, to the best of our knowledge, no proven method for tracking 6 d.o.f. rigid motion in CT coordinates during helical CT scanning has been published. Our aim in this work was to develop and evaluate such a method using a commercially available optical tracking system to enable future work on retrospective motion

correction methods. To obtain estimates of object motion in fixed CT coordinates, it is necessary to convert data provided by the motion tracker coordinates using a 4×4 calibration matrix, which describes the spatial relationship between the tracker and CT isocenter space. We describe two methods for obtaining this calibration matrix and validate these methods in actual CT scans of a 3D brain phantom.

II. METHODS

A. Data acquisition

An optical motion tracking system (Polaris Spectra Northern Digital Inc., Waterloo, Canada) was positioned at the rear of the scanner gantry. This system can report the six d.o.f. pose of multiple rigid targets comprising three or more retroreflective markers. A 3D Hoffman brain phantom[16] with an attached target comprising four retro-reflective disks (0.6 cm radius) was placed on the bed, and a further target with three disks was attached to the front end of the bed.

All tracker calibration matrices were derived from a series of six reconstructed helical CT scans (denoted $s1-s6$) of the phantom in different poses. CT scans were acquired on a Siemens Biograph 16 PET/CT scanner which incorporates a standard Siemens Somatom Sensation 16-slice CT scanner. The scan parameters were as follows: reconstruction matrix 512 × 512; slice thickness 1.0 mm; axial pitch 0.5; tube voltage 120 kVp; and the current varied from 75 mA to 480 mA using the manufacturer's dose reduction method. The reconstructed pixel size depended on the selected topogram and was $\leq$ 0.59 mm.

The tracker recorded poses of the phantom and bed at 60 Hz. The start and end of detected bed motion was used to synchronise with CT acquisition. Two further phantom scans in different poses were acquired for validation of motion estimates (Section II C). These were denoted $s7$ and $s8$. This procedure was repeated on four separate occasions (days 1 to 4).

B. Tracker Calibration

1. Converting between image and isocenter space

In CT, the center of the reconstructed image does not necessarily correspond to the scanner's isocenter as the scanning volume is operator-selectable. To calibrate the tracker and isocenter coordinate systems using reconstructed image data, the spatial relationship between the image and isocenter spaces must first be established. Image coordinates (i, j, k) were converted to isocenter coordinates, (P_x, P_y, P_z) using

$$\begin{array}{rcl} P_x &=& S_x + id_x, \quad \text{where} \quad S_x = -d_x(\frac{n_x-1}{2}) \\ P_y &=& S_y + jd_y, \quad \text{where} \quad S_y = -(\delta_y - h) \\ P_z &=& S_z + kd_z, \quad \text{where} \quad S_z = -d_z(\frac{n_z-1}{2}) \end{array} \qquad (1)$$

where $S_{x,y,z}$ are the isocenter coordinates of the top left voxel of slice 1; $d_{x,y,z}$ are the x, y and z voxel sizes, respectively, n_x and n_z are the x and z dimensions of the reconstructed image matrix, respectively; δ_y is the vertical distance from the top left corner voxel of the image volume to the upper surface of the bed; and h is the vertical distance between the isocenter and the upper surface of the bed, i.e. the bed height. All these parameters were obtained from the DICOM header.

2. Method I: Calibration by Absolute Orientation

Absolute orientation (AO) is the common problem of recovering the transformation between two different Cartesian coordinate systems using the estimated locations of a set of points in each coordinate system. We considered an individual marker attached to the Hoffman phantom, which was imaged in a different pose in each scan. Marker position in isocenter coordinates was obtained by locating its center in the reconstructed image and applying Eq. (1). The corresponding position in tracker coordinates was obtained as the mid-scan measurement, at which time the center of the total imaged volume (which moves with the patient bed during the scan) coincided with the isocenter. The transformation T_c relating the two coordinate systems was then found by applying a closed-form least squares method[17] to the paired coordinate measurements. A separate determination of T_c was performed using the data acquired on each of the four days.

3. Method II: Calibration by Image Registration

We also trialled a novel calibration method applied to the same CT scans. We grouped the reconstructed scans into 15 pairs. For each pair the scan-to-scan motion in tracker coordinates, M_T, was computed from tracker data. The corresponding motion in image space, M_R, was estimated using an automated 3D rigid registration algorithm, which used a cost function defined as the sum of squared differences between the pixel intensities. M_R was converted to its equivalent in isocenter coordinates, M_{R_I}, by accounting for the displacement of the image from the isocenter, given by Eq. 1.

TABLE I. RMS landmark position errors after transformation.

Day	Mean RMS error (mm)					
	AO-based calibration			IR-based calibration		
	x	y	z	x	y	z
1	0.71	1.03	0.00	0.45	0.38	0.00
2	0.94	0.59	0.21	0.48	0.41	0.21
3	0.48	0.76	0.44	0.43	0.45	0.25
4	0.56	0.38	0.00	0.25	0.45	0.03

Since the desired calibration matrix, T_c, converts between tracker coordinates and isocenter coordinates, differences between the motion in isocenter coordinates, M_{T_I}, estimated from motion tracker data as

$$M_{T_I} = T_c M_T T_c^{-1} \tag{2}$$

and the motion estimated by image registration, M_{R_I}, should be minimized by an accurate estimate of T_c. We therefore investigated the ability of an amoeba function minimization procedure to iteratively determine the six parameters of T_c from a series of registrations. These parameters were allowed to vary, and the cost function was the sum of the absolute differences between the six parameters of M_{T_I} and M_{R_I}. As in the AO method, four separate determinations of T_c were performed using the CT scan data acquired on four separate days.

C. Validating the Calibration Matrices

Calibration matrix accuracy was assessed using scans $s7$ and $s8$ acquired on each of the 4 days. For each pair of scans $s7$ was treated as a reference, and $s8$ was transformed by the inter-scan movement calculated using Eq. (2), where T_c was the calibration matrix obtained with either the AO or IR method. Alignment accuracy was estimated by (a) landmark analysis by three independent observers, where each observer estimated the 3D location of 12 well-spaced landmarks in the reconstructed images, from which RMS errors in x, y and z were calculated, and (b) by computing the correlation coefficient of all voxels within a 3D region of interest enclosing the phantom in the co-registered images. The correlation coefficient was expected to be the more reliable measure of alignment accuracy as it uses all voxels within the phantom and is non-subjective.

TABLE II. Effect of calibration method on registration accuracy.

Day	Correlation Between Reference and Transformed Images Mean (1 s.d.)	
	AO-based calibration	IR-based calibration
1	0.880 (0.004)	0.944 (0.002)
2	0.872 (0.010)	0.912 (0.009)
3	0.973 (0.001)	0.988 (0.001)
4	0.973 (0.001)	0.981 (0.001)

III. RESULTS

Results of landmark analysis (mean results for 3 observers) are shown in Table I. The largest positional error was $\simeq$1.0 mm (RMS), in the y direction. Errors were generally larger when the AO-based calibration was used. With IR-based calibration, all errors were less than 0.5 mm (RMS).

Table II shows linear Pearson correlation coefficients between ROI voxels in the reference and transformed images, averaged over ten adjacent slices, for each day and each calibration method. Images transformed using IR-based calibration matrices were consistently better correlated with the reference images. This can be seen graphically in correlation plots for a typical slice from Day 1 (Fig. 1). Less scatter about the line of identity was observed with IR-based calibration (Fig. 1(b)). The prominent deviations from the line of identity are attributed to some residual water which occupied different parts of the phantom in the two scans.

Noticeably better correlation was observed with both calibration methods on days 3 and 4. This may be due to the different motions applied to the phantom: the motions and in particular the rotations were smaller on day 3 and day 4, and correcting for a smaller motion is likely to yield smaller errors.

IV. DISCUSSION AND CONCLUSION

We have shown that rigid motion can be accurately estimated in isocenter coordinates during helical CT using a properly calibrated optical motion tracking system. The method requires a calibration matrix to convert pose estimates in tracker coordinates to isocenter coordinates. We compared two methods of determining this matrix, and observed that the new IR-based method was consistently more accurate than the conventional AO method. This may be because the IR method makes use of all voxels in the 3D image, whereas the AO method uses a

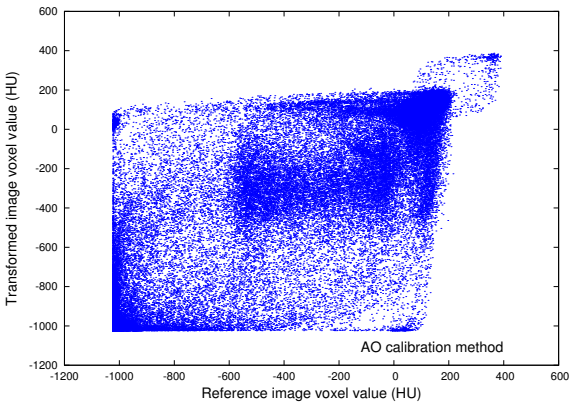

(a)

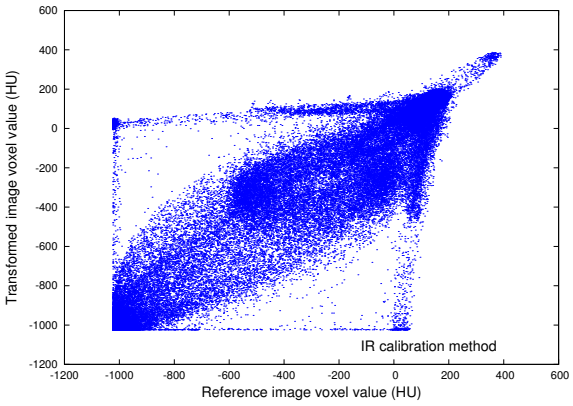

(b)

FIG. 1. Correlation between ROI voxel values in the reference and transformed images in a typical slice (Day 1). (a) Correlation between reference and transformed images using AO-based calibration; (b) Correlation between reference and transformed images using IR-based calibration.

limited number of fiducial points, the positions of which in image space are subjectively determined and limited in precision. Further, the IR method utilizes both rotational and positional parameters of object pose, whereas the AO method only considers position.

The IR method has the additional advantage that it can be completely automated after acquiring the required number of CT scans. Its simplicity and robustness may also be advantageous in other imaging modalities such as PET and SPECT where the AO method has become established.[18–23]

We repeated the calibration procedures on each scanning day, but for clinical studies we would use a reference target permanently attached to the scanner gantry to avoid the need to repeat the calibration procedure when the tracking system was moved.[20,23] These experiments used a physical phantom to which the motion tracking target was rigidly fixed, which avoided tracking errors due to non-rigid target fixation. In clinical studies, we will use similar target attachment methods to those used previously in PET.[19–22]

In summary, we have developed and demonstrated the feasibility of a simple, accurate and convenient rigid motion tracking method for helical CT. This represents an important step towards the development of methods to compensate for rigid head motion during helical CT scans in a clinical setting, and may also be useful for tracker calibration in other imaging modalities such as PET.[18–23]

ACKNOWLEDGMENTS

This work was supported by the National Health and Medical Research Council Project Grant 632677. J. Kim is supported by a University Postgraduate Award from the University of Sydney. We would like to acknowledge the staff of the Departments of Nuclear Medicine and Radiology, Westmead Hospital for their cooperation and assistance, in particular David Skerrett, Rochelle McCredie for participating in landmark analysis, Robert Barnett and Scott Evans for computing and technical support. We also thank Professor Harry Barrett of the University of Arizona for helpful discussions.

* roger.fulton@sydney.edu.au

[1] R. Popilock, K. Sandrasagaren, L. Harris, and K. A. Kaser, "CT artifact recognition for the nuclear technologist," *J. Nucl. Med. Technol.* **36**, 79–81 (2008).

[2] M. Yazdi and L. Beaulieu, "Artifacts in spiral x-ray CT scanners: Problems and solutions," *Int. J. Biol. Life Sci.* **4**(3), 135–139 (2008).

[3] S. Kaste, "Issues specific to implementing PET-CT for pediatric oncology: what we have learned along the way," *Pediatr. Radiol.* **34**, 205–213 (2004).

[4] B. Lee and A. Newberg, "Neuroimaging in traumatic brain imaging," *NeuroRx.* **2**(2), 372–383 (2005).

[5] G. Wang, and M. W. Vannier, "Preliminary study on helical CT algorithms for patient motion estimation and compensation," *IEEE Trans. Med. Imag.* **14**, 205–211 (1995).

[6] D. Schäfer, M. Bertram, N. Conrads, J. Wiegert, G. Rose, and V. Rasche, "Motion compensation for cone-beam CT based on 4D motion field of sinogram tracked markers," *Int. Congr. Ser.* **1268**, 189–194 (2004).

[7] H. Yu, and G. Wang, "Data consistency based rigid motion artifact reduction in fan-beam CT," *IEEE Trans. Med. Imag.* **26**, 249–260 (2007).

[8] M. W. Jacobson and J. W. Stayman, "Compensating for head motion in slowly-rotating cone beam CT sys-

tems with optimization transfer based motion estimation," 2008 IEEE Nuclear Science Symposium Conference Record, 5240–5245, (2008).

[9] U. K. Bhowmik, M. Z. Iqbal, and R. R. Adhami, "Mitigating motion artifacts in FDK based 3D cone-beam brain imaging system using markers," *Cent. Eur. J. Eng.* **2**(3), 369–382 (2012).

[10] C. Bodensteiner, C. Darolti, H. Schumacher, L. Matthäus, and A. Schweikard, "Motion and positional error correction for cone beam 3D-reconstruction with mobile C-arms," Med. Image Comput. Comput. Assist. Interv. Int. Conf. Med. Image Comput. Comput. Assist. Interv., **10**, 177–185, (2007).

[11] J. Nuyts, J.-H. Kim, and R. Fulton, "Iterative CT reconstruction with correction for known rigid motion," 11th International Meeting on Fully Three-Dimensional Image Reconstruction in Radiology and Nuclear Medicine, Potsdam, Germany, 132–135, (2011).

[12] S. Zafar, "Post scan correction of step, linear and spiral motion effects in CT scans," *Int. J. Comput. Appl.* **35**(10), 13–19 (2011).

[13] B. Westermann and R. Hauser, "Online head motion tracking applied to the patient registration problem," *Comp. Aid. Surg.* **5**, 137–147 (2000).

[14] A. Wagner, K. Schicho, F. Kainberger, W. Birkfellner, S. Grampp, and R. Ewers, "Quantification and clinical relevance of head motion during computed tomography," *Invest. Radiol.* **38**, 733–741 (2003).

[15] A. Katsevich, M. Silver and A. Zamyatin, "Local tomography and the motion estimation problem," *SIAM J. Imaging Sciences* **4**, 200–219 (2011).

[16] E. J. Hoffman, P. D. Cutler, W. M. Digby, and J. C. Mazziotta, "3-D phantom to simulate cerebral blood flow and metabolic images for PET," *IEEE Trans. Nucl. Sci.* **37**(2), 616–620 (1990).

[17] B. K. P. Horn, "Closed-form solution of absolute orientation using unit quaternions," *J. Optical Soc. Amer.* **4**, 629–642 (1987).

[18] R. Fulton, S. Eberl, S. Meikle, B. Hutton, and B. Braun, "A practical 3D tomographic method for correcting patient head motion in clinical SPECT," *IEEE Trans. Nucl. Sci.* **46**(3), 667–672 (1999).

[19] B. Lopresti, A. Russo, W. F. Jones, T. Fisher, D. G. Crouch, D. Altenberger, and D. W. Townsend, "Implementation and performance of an optical motion tracking system for high resolution PET brain imaging," *IEEE Trans. Nucl. Sci.* **46**, 2059–2067 (1999).

[20] R. Fulton, S. Meikle, S. Eberl, J. Pfeiffer, C. Constable, and M. Fulham, "Correction for head movements in positron emission tomography using an optical motion tracking system," *IEEE Trans. Nucl. Sci.* **49**(22), 116–123 (2002).

[21] P. M. Bloomfield, T. J. Spinks, J. Reed, L. Schnorr, A. M. Westrip, L. Livieratos, R. Fulton, and T. Jones, "The design and implementation of a motion correction scheme for neurological PET," *Phys. Med. Biol.* **48**, 959–978 (2003).

[22] P. J. Noonan, J. Howard, J. Anton-Rodriguez, T. F. Cootes, W. A. Hallett and R. Hinz, "Image space identification of a motion tracking tool in PET and PET/CT," 2010 IEEE Nuclear Science Symposium/Medical Imaging Conference (NSS/MIC), 2681–2686 (2010).

[23] A. Kyme, V. Zhou, S. Meikle, and R. Fulton, "Real-time 3D motion tracking for small animal PET," *Phys. Med. Biol.* **53**, 2651–2666 (2008).